

Elastic moduli for a diblock copoly(2-oxazoline) library obtained by high-throughput screening

Johannes M. Kranenburg,^a Catherine A. Tweedie,^b Richard Hoogenboom,^a Frank Wiesbrock,^a Hanneke M. L. Thijs,^a Chris E. Hendriks,^a Krystyn J. Van Vliet^b and Ulrich S. Schubert^{*a}

Received 7th February 2007, Accepted 27th March 2007

First published as an Advance Article on the web 23rd April 2007

DOI: 10.1039/b701945a

Using depth-sensing indentation, the elastic modulus E of a diblock copoly(2-oxazoline) library was investigated in order to determine structure–property relationships. The adopted experimental procedure, dropcasting of the copolymer materials and determining the elastic modulus by depth-sensing indentation, was compatible with high-throughput experimentation. The elastic modulus of the investigated materials depended strongly on the side-group. Materials containing poly(nonyloxazoline) exhibited a lower modulus than materials without any poly(nonyloxazoline) block as poly(nonyloxazoline) was at room temperature above its glass-transition temperature T_g , while the other homopolymers in this study were glassy at room temperature. The elastic modulus also depended on the relative humidity (RH) of the testing environment; the stiffness of ethyloxazoline and methyloxazoline decreased significantly due to water absorption from the air. At lower RH, hydrogen bonding or polar interactions among the polymer chains resulted in a surprisingly high modulus for the poly(methyloxazoline). In addition, as anticipated, the elastic moduli of AB diblock copolymers were bounded by those of the A and B homopolymers, both at high and at low RH. The presented results indicate how, and to what extent, for these materials the E (and the change in E) at a given (change in) humidity can be adjusted by tailoring the composition.

Introduction

High-throughput experimentation (HTE) encompasses automated and preferably parallel synthesis and characterization. HTE is a powerful tool to explore large parameter spaces and to identify structure–property relationships.^{1,2} Depth-sensing indentation is a suitable experimental approach for high-throughput probing of mechanical properties such as the elastic modulus E and creep compliance.^{3,4} During depth-sensing indentation, also called instrumented indentation or nanoindentation, the load applied by a rigid indenter on the material surface and the penetration depth into the material surface are measured simultaneously.^{5,6} The technique provides the advantages of requiring only small amounts of sample material and of allowing automated, sequential measurements over one or many samples.^{3,4}

From the reaction of nitriles with 2-aminoethanol, a large number of differently substituted 2-oxazolines can be prepared that are well-suited monomers for living cationic ring-opening polymerizations.^{7,8} ‘Living’ polymerization implies that the growth of all polymer chains starts at the same time, that all polymer chains grow with uniform speed and that chain-transfer reactions, terminating reactions, as well as other side-reactions are absent. Therefore, the molecular weight

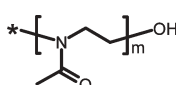
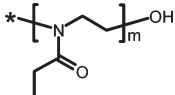
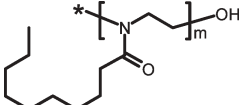
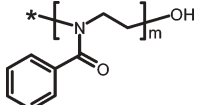
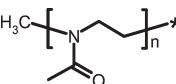
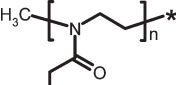
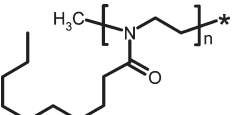
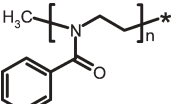
distribution of the resulting polymer is narrow and the reaction centers remain active after the complete consumption of the first type of monomer, allowing the subsequent incorporation of a second monomer type into the polymer chains. Thus, diblock copoly(2-oxazoline)s with a narrow molecular weight distribution can be obtained in a two-step procedure.

Recently, we have shown that the comparably long reaction times for the polymerization of 2-oxazolines, which has often been a major concern in this research area, can be reduced by performing the reactions at higher temperatures.^{9–11} Utilizing 2-methyl-, 2-ethyl-, 2-nonyl- and 2-phenyl-2-oxazoline as monomers, a 16-membered library of 12 diblock copolymers and 4 chain-extended homopolymers were synthesized in a microwave reactor (Table 1).⁹ These compounds showed only slight deviations from the targeted composition of 50 + 50 monomer units, and had narrow molecular weight distributions, as indicated by the polydispersity index (PDI) being smaller than 1.2. The two exceptions that show a higher PDI, NonMe and NonEt (abbreviations as in Table 1), are discussed elsewhere.⁹ Differential scanning calorimetry (DSC) demonstrated that the glass-transition temperature T_g of these materials depended on the side group (Table 1). No glass-transition temperature was observed for the chain-extended poly(nonyloxazoline). Probably due to insufficient instrument resolution, no T_g was observed for PheNon and NonPhe, either. All polymers that contained (at least) one block of poly(nonyloxazoline) had a melting temperature T_m in the range of 146 to 151 °C, whereas all other polymers were fully amorphous to the extent detectable *via* DSC.⁹ The

^aLaboratory of Macromolecular Chemistry and Nanoscience, Eindhoven University of Technology and Dutch Polymer Institute (DPI), P.O. Box 513, 5600 MB, Eindhoven, The Netherlands. E-mail: u.s.schubert@tue.nl; Fax: (+31) 40 247 4186

^bLaboratory for Material Chemomechanics, Massachusetts Institute of Technology, 77 Massachusetts Avenue, Cambridge, MA, USA

Table 1 Overview of the 16-membered set of diblock copoly(2-oxazoline)s and chain-extended homo poly(2-oxazoline)s, showing the abbreviation, the degree of polymerization for the first and the second block, and the glass-transition temperature for each compound (data from ref 9)

| Second block → First block ↓ |  |  |  |  |
|--|---|---|--|---|
| | Poly(2-methyl-2-oxazoline) | Poly(2-ethyl-2-oxazoline) | Poly(2-nonyl-2-oxazoline) | Poly(2-phenyl-2-oxazoline) |
|  Poly(2-methyl-2-oxazoline) | MeMe 50 : 50 79 °C | MeEt 50 : 49 63 °C | MeNon 50 : 52 69 °C | MePhe 50 : 52 88 °C |
|  Poly(2-ethyl-2-oxazoline) | EtMe 50 : 50 69 °C | EtEt 50 : 50 59 °C | EtNon 50 : 50 60 °C | EtPhe 50 : 52 89 °C |
|  Poly(2-nonyl-2-oxazoline) | NonMe 50 : 50 71 °C | NonEt 50 : 46 56 °C | NonNon 50 : 50 — | NonPhe 50 : 45 — |
|  Poly(2-phenyl-2-oxazoline) | PheMe 50 : 48 92 °C | PheEt 50 : 46 84 °C | PheNon 50 : 50 — | PhePhe 50 : 50 107 °C |

surface energy, determined by contact-angle measurements of diiodomethane and ethyleneglycol droplets on films of these copolymers, was 43 to 46 mN m⁻¹ if the polymers did not contain any poly(nonyloxazoline).¹² For polymers that contained (at least) one block of poly(nonyloxazoline), the surface energy was lower (19 to 23 mN m⁻¹) due to close packing of the nonyl side groups at the surface. Atomic force microscopy (AFM) imaging of spin-cast films demonstrated a higher roughness if the polymers contained at least one block of poly(nonyloxazoline), as compared to films without any poly(nonyloxazoline).¹³ The syntheses, the thermal characterization as well as the surface energy measurements of this library of diblock copolymers were performed in a manner compatible with high-throughput experimentation.^{9,12}

The control over molecular weight, side groups, and side-group distribution within the chains, which is typical for these polymers and this synthesis method, provides tunability of the physical properties. Additionally, this control over molecular structure and the narrow molecular weight distribution make them suitable materials to study quantitative structure–property relationships. In view of potential application of poly(oxazoline)s as, *e.g.* active components in hair-dressing formulations or impregnants for paper or textiles,^{14–16} the mechanical properties deserve to be studied as well. Until recently, the study of the mechanical properties of poly(oxazoline)s has been limited to peel tests that use mechanical force to separate a film from the underlying substrate,^{17–19} as well as a few rheological measurements of complex shear

moduli,²⁰ dynamic mechanical analysis, and uniaxial tensile tests of freestanding films.²¹

In the present study, *E* of diblock copoly(oxazoline)s is studied using depth-sensing indentation, and structure–property relationships are discussed. As the relative humidity (RH) of the testing environment influenced *E*, measurements were repeated on all materials at three RH levels. The current study expands the applicability of depth-sensing indentation for high-throughput experimentation by combining the freedom in the selection of the starting materials in the approach of Tweedie *et al.*⁴ with the concept of preparing the samples from a polymer solution of Simon *et al.*²²

Experimental

Preparation of the library

Diblock copoly(2-oxazoline)s have been prepared *via* cationic ring-opening polymerization.⁹ The diblock copoly(oxazoline)s, their abbreviations and the glass-transition temperatures (measured by DSC)⁹ are listed in Table 1. Twenty (20) mg of each copolymer was dissolved in 50 μL of chloroform (Biosolve LTD), except for the chain-extended poly(methyl-oxazoline), MeMe, which did not dissolve in chloroform at this concentration and was dissolved in demineralized water. After complete dissolution, approximately 5 μL from each solution was pipetted onto a glass slide (Marienfeld, Lauda-Königshofen, Germany), with a nominal center-to-center spacing of 4 mm between polymer spots. Four such glass

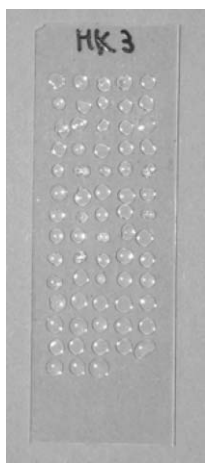


Fig. 1 One of the four prepared glass slides with dropcasted samples. The first three rows and the first spot of the fourth row form the diblock copolymer library that is discussed in this article.

slides were prepared, one of which is shown in Fig. 1. The first three rows and the first spot of the fourth row form the library discussed in this article. The diameter and the height (after 2 days drying under ambient conditions) of the spots ranged from approximately 2 to 3.5 mm, and from 100 to 400 μm , respectively, as measured with an optical profilometer (Fogale Zoomsurf) and a mechanical profilometer (Tencor P10). Only the chain-extended methyloxazoline sample, MeMe, had a significantly lower thickness (50 μm) due to the alternative solvent used.

Accurate determination of the elastic modulus from the indentation load-displacement responses requires flat sample surfaces.²³ Profilometry showed that this condition was met for indentations near the middle of the polymer spots. After deposition onto the glass slide, one library was dried at ambient conditions for four days, dried for four hours at 40 $^{\circ}\text{C}$, and subsequently dried at 45 $^{\circ}\text{C}$ under vacuum overnight prior to the indentation measurements using a commercial indentation instrument (Nanotest600, Micro Materials LLC, Wrexham, UK). Two additional copies of the library were dried for three weeks at ambient conditions and another three weeks at 40 $^{\circ}\text{C}$ under vacuum, and then transferred to a different commercial indentation instrument (TriboIndenter, Hysitron, Inc., MN, USA) for testing. The samples resided at low humidity (<7%) for one week before testing at 5.4% relative humidity. After the experiments at low RH, the relative humidity was raised to 40% RH and two weeks later the measurements were repeated.

Reference samples

In addition, two reference samples were prepared: a phenyloxazoline-ethyloxazoline (PheEt) diblock copolymer that was dropcast on a separate glass slide and then annealed above the corresponding T_g , and a chain-extended nonyloxazoline homopolymer (NonNon) that was compression molded and then heated above the corresponding melting temperature on a separate glass slide. The surface roughness of these reference samples that were processed at relatively high temperature was expected to be greater than that of the library samples.

Tapping mode atomic force microscopy (AFM) indicated that even the reference samples possessed relatively smooth surfaces, although the PheEt reference sample surface exhibited some randomly dispersed protrusions (spaced $\sim 1.5 \mu\text{m}$ apart, surface to peak height <29 nm and R_a of 0.85 nm) and the NonNon reference sample surface exhibited randomly dispersed pits (spaced $\sim 1 \mu\text{m}$ apart with a surface-to-pit amplitude of <40 nm and R_a of 3.8 nm). These surface conditions may cause minor errors (<5%, in the worst case of indenting precisely on top of a protrusion or in a pit <10%) for the shallowest indents resulting from the lowest maximum loads.²⁴ For deeper indents these errors quickly diminish. A fortunate detail is that NonNon, the sample with the greatest surface roughness, has a low E and therefore relatively deep indents (>400 nm) even at the lowest maximum load.

Depth-sensing indentation

Indentation experiments were conducted on two instruments: a NanoTest600 (Micro Materials LLC, Wrexham, UK, maximum force of 35 mN at NT1 gain settings) and a TriboIndenter (Hysitron, Inc. Minneapolis, MN, USA, maximum force of 10 mN).

The humidity in the NanoTest600 indenter case was regulated by flushing with nitrogen gas and by pumping the air-nitrogen mixture from the indenter case through a tube of desiccant. During the measurements, the relative humidity (RH) was maintained at $9.0 \pm 0.8\%$ via the nitrogen flow only, to avoid noise due to the circulation pump, while the temperature was maintained at 25 $^{\circ}\text{C}$. The indentations were executed in load-control mode, with a loading time, hold time at maximum load, and an unloading time of 2 s, 10 s and 1 s, respectively. For visco-elastic materials, such a combination of a hold time and a quick unloading is necessary for determining E .^{25,26} No thermal drift correction was applied as thermal drift is typically very small ($\sim 0.01 \text{ nm s}^{-1}$) for this instrument. Three indentations to 2 mN maximum load were made per sample at an optically inspected position on every polymer spot where the surface appeared smooth and perpendicular to the loading direction. Measurements were performed using a rounded conical, diamond indenter with an effective radius of 4.1 μm . For several samples, indentations with a Berkovich (trigonal pyramid) indenter were made as well. On the MeMe sample, profile scans of the residual indentations were made using the NanoTest600; the indenter tip scanned the surface with 50 μN topography load and 0.25 $\mu\text{m s}^{-1}$ scanning velocity.

The indentation experiments with the TriboIndenter were performed at $5.4 \pm 0.4\%$ and $40 \pm 1\%$ RH with a diamond Berkovich indenter. Before every indent, the indenter was held in contact with the surface, to allow for piezoactuator stabilization (35 s) and drift correction (40 s), at a contact load of only 0.5 μN to prevent any deformation prior to the indentation experiment. The drift rate (typically 0.1 nm s^{-1}) was automatically determined over the last 20 s of the 40 s period. After lifting the tip 30 nm and reapproaching the surface (surface detection at a load of 0.5 μN), the tip was loaded to maximum load in 10 s, held at maximum load for 10 s and unloaded in 2 s. The maximum load was reduced in

steps of 300 μN from 3 mN to 300 μN . From the 10 measurements (spaced 50 μm apart) per sample, the first two were left out from the analysis to even further reduce the influence of drift. On the MeMe and MeEt samples, residual indents were imaged upon full unloading of the surface using the TriboIndenter Berkovich diamond indenter as a contact profilometer with a preload of 0.5 μN .

Analysis

Load-displacement responses were analyzed *via* the method of Oliver and Pharr⁵ by fitting the unloading response from 0.95 P_{max} to 0.20 P_{max} with the conventional power law form to obtain the slope at the start of the unloading S . From the slope S and the maximum depth h_{max} , the contact depth h_{c} is determined using:

$$h_{\text{c}} = h_{\text{max}} - 0.75 \frac{P_{\text{max}}}{S} \quad (1)$$

The projected contact area as a function of contact depth (the ‘area function’) was determined by prior indents on quartz, the standard reference material. For the TriboIndenter, this area function was extended to larger distances from the tip apex than could be reached on quartz by indentations on polycarbonate. From the area function and the contact depth h_{c} the projected contact area A can be calculated. With $\beta = 1$, the reduced modulus E_{r} is then calculated as:

$$E_{\text{r}} = \frac{\sqrt{\pi}}{2\beta} \cdot \frac{S}{\sqrt{A(h_{\text{c}})}} \quad (2)$$

The reduced modulus takes into account that elastic displacements occur both in the specimen (with modulus of elasticity E_{sample} and Poisson’s ratio ν_{sample}) and in the indenter:

$$E_{\text{r}} = 1 / \left(\frac{1 - \nu_{\text{sample}}^2}{E_{\text{sample}}} + \frac{1 - \nu_{\text{indenter}}^2}{E_{\text{indenter}}} \right) \quad (3)$$

Occasionally, an indentation response was neglected from analysis due to local surface imperfection-induced deviation from the other responses measured on the same sample. The error bars present one standard deviation out of eight or seven (TriboIndenter) and three (NanoTest600) measurements, unless otherwise stated.

Thermal gravimetric analysis

Thermal gravimetric analysis was conducted (Netzsch TG209 F1) at a heating rate of 20 K min^{-1} on 5 to 10 mg of selected diblock copolymer materials. These samples, which were taken from storage vials that were not hermetically sealed, were not dried before the TGA experiments. These materials are assumed to be equilibrated with ambient humidity.

Results and discussion

Method validation

A sixteen-membered library of copoly(oxazoline)s was characterized by depth-sensing indentation (DSI). As examples,

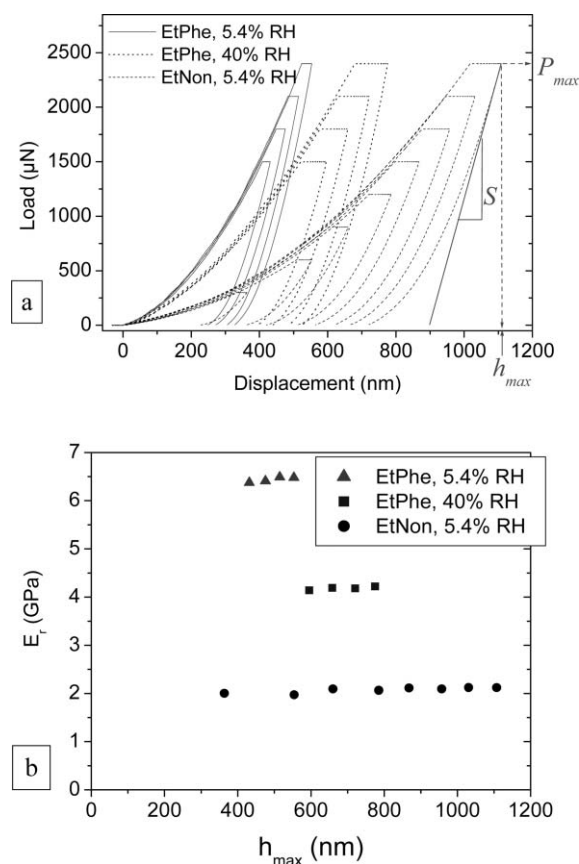


Fig. 2 (a) Indentation load-displacement responses (Berkovich indenter) and (b) analysis results for EtPhe at two humidities (5.4% and 40% RH) and for the EtNon copolymer, showing that higher humidity lowers the stiffness of the material, and that EtPhe is stiffer than EtNon; for clarity, only four of the EtPhe responses are shown; key parameters for the calculation of E_{r} are displayed.

load-displacement responses obtained with a Berkovich indenter on the EtPhe and the EtNon diblock copolymers and the corresponding analysis results are shown in Fig. 2a and b, respectively. Key parameters from eqn (1) and (2) are indicated for one load-displacement response of EtNon. The EtPhe responses are much stiffer (have a higher E_{r} , see Fig. 2b) than the EtNon. At higher RH, the stiffness of EtPhe is reduced, as can be observed visually in the loading response. The creep during the hold time increases as well.

Fig. 3 shows results on reference materials that were processed such that the material contained no solvent; PheEt was annealed above its T_{g} and NonNon was melt processed. The E_{r} of these samples corresponded well with those on the corresponding samples from the HTE library. This shows that the chloroform from the dropcasting is absent or its amount is so reduced that its effect on E_{r} can be neglected. The thick NonNon reference sample appeared white due to crystallization, while the corresponding sample from the library was transparent, due ostensibly to the smaller crystallite size. Nevertheless, the moduli of both poly(nonyloxazoline) samples were nearly identical ($E_{\text{r,meltprocessed}} = 0.96 \text{ GPa}$; $E_{\text{r,library}} = 1.03 \text{ GPa}$).

For some of the tested materials (for instance EtEt), sample preparation and tensile testing are very difficult due to the

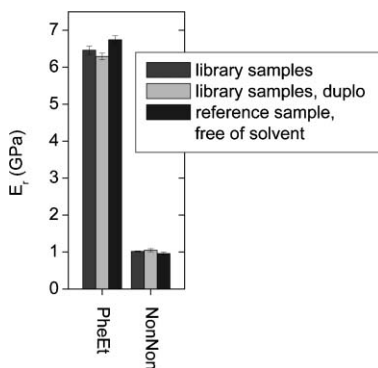


Fig. 3 Comparison of library samples with solvent-free reference samples (Berkovich tip, TriboIndenter, 5.4% RH).

brittleness of these materials.²¹ However, DSI measurements could be performed successfully, resulting in small standard deviations in measurements on the same sample, and in good agreement between duplicate samples (Fig. 4). The high-throughput nature of the measurements is illustrated using a measurement series performed with the TriboIndenter; ten measurements per copolymer spot were performed on two slides with sixteen copolymer spots each. These 320 measurements were performed in an automated run for 20 hours, of which 11 hours were spent on moving to the next indent position and approaching the sample surface between two indents. These 11 hours may be reduced by performing a quick

approach to the sample surface at each spot near the indent positions before starting the actual measurement. This run was not fully optimized for this potential increase in experimental throughput.

Chain-extended homopolymers

Results from the load-displacement responses of the entire library samples are presented in Fig. 4a–c. The results in Fig. 4a and c are obtained with the TriboIndenter on two sample slides and at two humidity levels, and the results in Fig. 4b are obtained at an intermediate RH using the NanoTest600. At low RH, the elastic modulus of the nonyloxazoline homopolymer ($E_r = 1.03$ GPa) was lower than E_r of the other homopolymers. Differential scanning calorimetry (DSC) demonstrated that for MeMe, EtEt and PhePhe, T_g is above room temperature (Table 1). With increasing side-chain length (methyl, ethyl,⁹ propyl, pentyl)²⁷ T_g decreases. No T_g was observed for heptyloxazoline and nonyloxazoline homopolymers.²⁷ Though the exact location of T_g of NonNon could not be determined, it is expected to be lower than the T_g of pentyloxazoline homopolymer, *i.e.* lower than 5 °C. Pentyloxazoline, heptyloxazoline and nonyloxazoline homopolymers exhibit a melting temperature near 150 °C.²⁷ The observed E_r of NonNon is in the range expected for semi-crystalline polymers probed at a temperature between T_m and T_g . As NonNon is not glassy, it has a lower modulus than MeMe, EtEt and PhePhe (Fig. 4a and b) but the

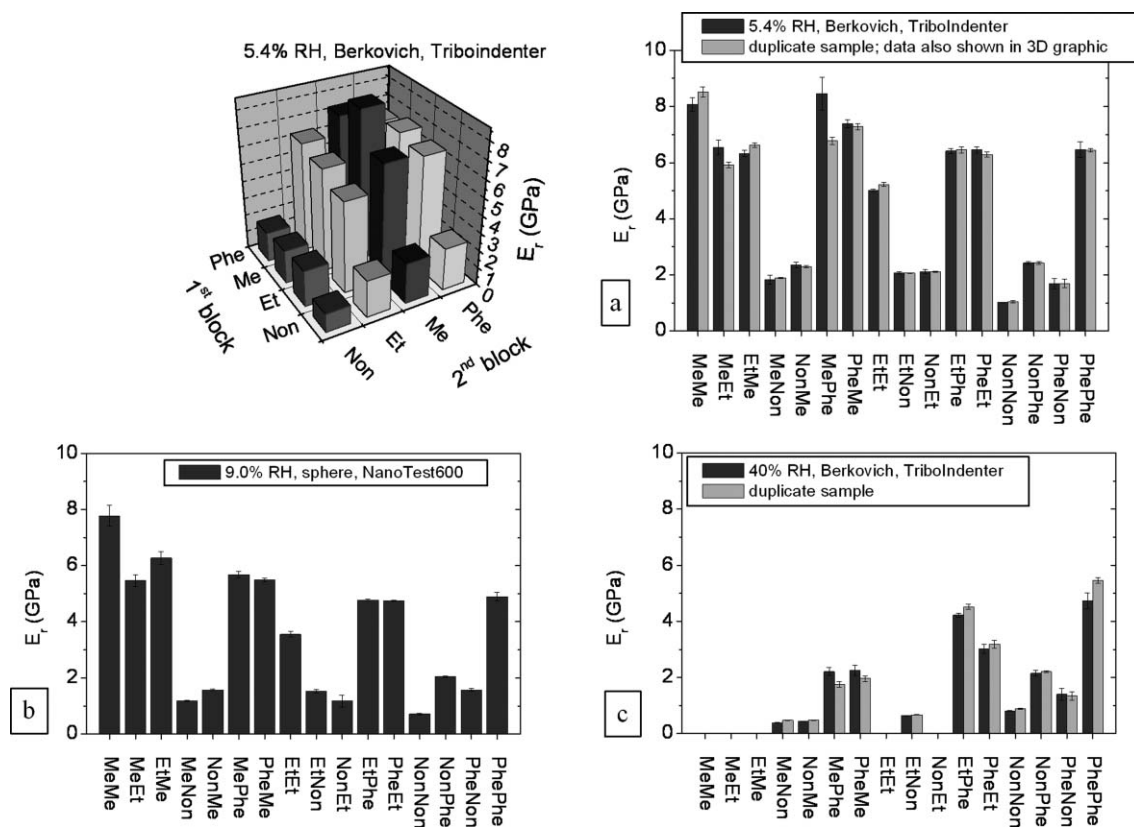


Fig. 4 Depth-sensing indentation results obtained at different humidities and with two indenter geometries (a and c, Berkovich; b, indenter with spherical apex); symmetry in reduced moduli (5.4% RH) is visualized in the 3D graphic; indents outside the tip-shape calibration range and indents with a high creep rate are disregarded.

semicrystallinity of the poly(nonyloxazoline) prevents E_r from dropping to the MPa range (the MPa range is typical for amorphous polymers above T_g).

EtEt ($E_r = 5.1$ GPa, Fig. 4a) has a lower E_r than MeMe (8.2 GPa) and PhePhe (6.5 GPa). MeMe and EtEt are both hygroscopic. The low elastic modulus of EtEt can be explained by some water that is present in the sample even at 5.4% RH. For hygroscopic polymers, water decreases the T_g and the elastic modulus of the glassy state.²⁸ This decrease of the modulus is most pronounced when (due to this decrease) T_g is (starts to be) close to the temperature at which the test is performed (*i.e.* room temperature). The decrease of the modulus due to water is most probably largest for EtEt, as at room temperature EtEt (free of water) is only 34 °C below its T_g ,^{9,21} compared with 54 °C for MeMe (Table 1). Further indication that the difference between the glass-transition temperature T_g and room temperature influences the elastic modulus is given by the E_r of the EtPhe and PheEt samples, that are much closer to the E_r of PhePhe than to EtEt, corresponding to a much larger difference between their T_g and room temperature than for EtEt.

Apart from this, differences in intermolecular interactions and the occurrence of secondary glass transitions may result in different elastic moduli for MeMe, PhePhe and EtEt. Due to such a secondary glass transition, E is for instance ~ 2.5 GPa for polycarbonate, compared to ~ 3.3 GPa for polystyrene.^{29,30} Nuño-Donlucas *et al.* measured, *via* DMTA, a secondary transition for poly(ethyloxazoline) at -100 °C.²¹ If such transitions are absent for poly(methyloxazoline) and poly(phenyloxazoline), or are less effective in reducing E_r , this could be a second explanation as to why EtEt has a lower E_r than MeMe and PhePhe at 5.4% RH.

E_r of MeMe at low RH is surprisingly high (8.3 GPa) – significantly higher than that of PhePhe ($E_r = 6.5$ GPa, PhePhe is at room temperature 80 °C below T_g) and much higher than E_r typically measured with depth-sensing indentation on a stiff glassy polymer such as polystyrene.³¹ This high elastic modulus of MeMe is not due to experimental artifacts, as will be discussed in detail in the next paragraph. Another glassy polymer exhibiting an exceptional high E_r (9.5 to 15 GPa) is poly(acrylic acid).^{32,33} Such a high E_r indicates intermolecular interactions additional to the Van der Waals interactions. For poly(acrylic acid), these intermolecular interactions may arise from hydrogen bonds, while for poly(oxazoline)s, hydrogen bonds or polar interactions may play a role. Due to steric or chemical factors, for the polymers in this study, these interactions were strongest for poly(oxazoline)s with only a small methyl side group. Protons from water may hydrogen bond with the electronegative oxygen atoms of the poly(oxazoline). These water molecules may be attracted by the material from the surrounding atmosphere (as discussed later in this paper), and may be so tightly bound that they remain in the material even after the rigorous drying procedure. Two hydrogen bonds per water molecule result in intermolecular interaction between polymer chains. FTIR experiments (not shown) on the dried homopolymers demonstrated that the carbonyl peak of MeMe, EtEt and PhePhe was located at ~ 1626 cm^{-1} , while the carbonyl peak of NonNon was located at 1640 cm^{-1} . The first wavenumber (1626 cm^{-1})

matches the wavenumber attributed to hydrogen-bonded carbonyls in poly((hydroxyalkyl)oxazoline), while the carbonyl peak of NonNon is located close to the ‘free’ C=O position.¹⁸ Moreover, a larger signal in OH-stretching region (3400 – 3600 cm^{-1}) was observed for the MeMe, EtEt and PhePhe materials than for the NonNon material, indicating that the NonNon contains less moisture than the other three homopolymers. The presence of moisture may assist polar interactions between chains induced by $\text{N}-\text{C}=\text{O} \leftrightarrow \text{N}^+=\text{C}-\text{O}^-$ isomerism; such isomerism is inferred in the literature for poly(methyloxazoline).²⁰ In conclusion, the high E of MeMe is attributed to interchain interactions arising from hydrogen bonding and/or polar interactions.

Inquiry into experimental factors that may cause high E_r

The oxazoline materials in the current study are rather difficult to measure in macroscopic mechanical tests due to their brittleness. However, using depth-sensing indentation, the materials could be characterized successfully. The reduced elastic modulus E_r from depth-sensing indentation experiments on polymers is usually somewhat higher than E determined in macroscopic mechanical tests due to deviations from ideal viscoelastic behavior⁶ and pile-up (material heaps up next to the indent and causes an underestimation of the projected contact area, eqn (2), and therefore an overestimation in E_r).³⁴ Furthermore, as the diamond indenter is very stiff ($E_{\text{indenter}} \gg E_{\text{sample}}$) and the Poisson’s ratio ν is approximately 0.35 for most polymers in the class considered here,²⁹ eqn (3) shows that E_r is higher than the modulus of elasticity E of the polymers (for a high but reasonable $\nu = 0.4$ and $E_{\text{indenter}}/E_{\text{sample}} = \infty$, E_r is 19% higher than E). These three factors result for a reference material like polycarbonate in a difference between E and E_r of approximately 1 GPa ($E_r = 3.5$ GPa; $E \sim 2.5$ GPa).²⁹ The amount of pile-up observed during line scanning (NanoTest600) and profilometric imaging (TriboIndenter) of the indents on the MeMe was small (the resulting overestimation in E_r is $<8\%$). Substrate effects (*i.e.* the elastic properties of the substrate influencing the obtained results due to insufficient sample thickness with respect to the indentation depth) can safely be ignored; the MeMe sample had a thickness of 50 μm , while the deepest indent for this material in Fig. 4a was only 0.49 μm . Formation of a pre-indent (resulting in an artificially low measured contact depth and therefore an erroneously high E_r) can be excluded as well. The residual indentation observed after loading to a magnitude twice that of the preload was insignificant, and E_r of MeMe did not decrease with maximum load applied during the experiment (the effect of a pre-indent on the calculated E_r will decrease for deeper indents, resulting in a decreasing trend in E_r as a function of maximum load). In summary, the high reduced modulus E_r for MeMe, as compared to stiff glassy polymers such as polystyrene, appears to accurately reflect the significant stiffness of this polymer.

AB and BA diblock copolymers

The E_r of any AB diblock copolymer in this library is intermediate to that of the chain-extended A- and the B-polymers (Fig. 4). We observed that E_r of the diblock

copolymers with only one poly(nonyloxazoline) block was closer to E_r of NonNon than to that of the other (high T_g) component. Because the volume fraction of Non is large (volume fraction of Non is estimated to be $>60\%$ because of its long side-chain), the high T_g block has less influence on the resulting elastic properties. Furthermore, the volume fraction of the glassy phase is lower than the actual volume fraction of the high T_g component, as poly(nonyloxazoline) chains may surround segments of the high T_g component and thus provide them some freedom to move, resulting in non-glassy behavior of those high T_g segments.

The E_r of pairwise combinations (AB vs. BA) typically agreed very well with each other (Fig. 4). Only the diblocks with Non as the first block showed (in two out of three cases) a higher E_r than the pairwise combination ($E_{r,NonPhe} > E_{r,PheNon}$ and $E_{r,NonMe} > E_{r,MeNon}$). Chain transfer and chain coupling occurred to some extent during the synthesis of the NonMe, NonEt (and NonPhe).⁹ Therefore, the pairwise combinations differ in chain length, chemical composition distribution over the chains,⁹ structural morphologies as observed by AFM on films¹³ and mechanical properties. Fig. 4 a shows for nearly all samples a good agreement between duplicate experiments on spots of the same (co)polymer material on two different glass slides. Only for MePhe, this agreement is somewhat poorer. This is thought to be due to slightly poorer surface conditions for one of the MePhe samples. The lower E_r in Fig. 4a for MePhe, which also shows the lowest standard deviation, is probably most reliable.

Effect of humidity on E_r

For all samples considered, E_r decreased with increasing humidity (Fig. 4 and Fig. 5), the least humidity-sensitive samples being NonNon, NonPhe and PheNon. PhePhe was somewhat sensitive to humidity (1.3 GPa decrease for the increase in relative humidity from 5.4 to 40% RH). The

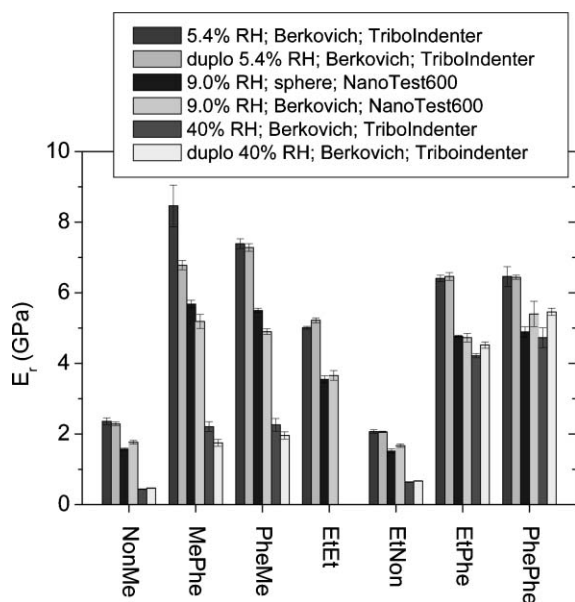


Fig. 5 Comparison of E_r obtained at several humidity levels and with two types of indenters for several selected samples.

Et and Me combinations with Non or with Phe were considerably more compliant with increasing humidity. The most humidity-sensitive samples were the EtEt, MeMe, MeEt and EtMe. At 40% RH for nearly all employed maximum loads, the displacement of the MeMe and EtEt surfaces exceeded the measurable depth range of the TriboIndenter (approximately 4.5 μm at the current settings). Van Caeter²⁰ reports $G' = 0.002$ GPa and $G''/G' \sim 0.2$ for chain-extended poly(methyloxazoline) from rheometry at 1 Hz and 40 °C. Assuming that Van Caeter conducted his experiments at ambient humidity, this result (particularly the high G''/G' ratio) corresponds qualitatively with the appreciable compliance of MeMe at ambient humidity (Fig. 4c).

The Oliver and Pharr analysis gives erroneous results if at the end of the hold period the creep, *i.e.* the displacement at sustained maximum load, is relatively high.²⁶ Therefore, if the ratio of the displacement rate at the start of the unloading over the displacement rate at the end of the hold period was smaller than 5 (an arbitrary criterion we have adopted), no results are given in Fig. 4 c. This was observed at 40% RH for the MeEt, EtMe and NonEt. Other diblocks that showed an appreciable but lower creep rate than the disregarded diblocks were EtNon, PheEt, EtPhe, PheMe, MePhe, NonMe and MeNon. (Furthermore, for EtNon, NonMe and MeNon the average and standard deviation presented in Fig. 4c is based on only four load-displacement responses as, due to larger deformation at increased humidity, only those responses remained within the tip-area function calibration.) For these samples, the presented E_r may exhibit a small error due to the creep. Also for EtEt at 9% RH, the E_r may be slightly affected, as the displacement rate at the start of the unloading was only 7 times the creep rate at the end of the hold period. For all other results presented in Fig. 4, this error source can be neglected.

The modulus of diblocks with Et, Me (and Phe) is affected by humidity. This corresponds with the observation that these materials, after equilibrating with ambient humidity, lose weight (Table 2) that can be attributed to water loss, when the material is heated during a TGA measurement (degradation of these polymers typically occurs at much higher temperatures, >350 °C).⁹ The relatively small decrease of E_r for PhePhe with increasing humidity can be explained by the high glass-transition temperature; therefore, in spite of the water present, the material remains glassy. The weight loss of the NonNon was much smaller. The stiffness of MePhe and PheMe decreased much more with increasing humidity than did the stiffness of EtPhe and PheEt (Fig. 4 and 5); this is explained by their respective water content at ambient humidity (Table 2).

Table 2 Weight loss during thermal gravimetric analysis (TGA) between 80 °C and 140 °C on selected (co)polyoxazoline materials that were prior to TGA measurements approximately in equilibrium with ambient humidity

| Material | Weight loss (%) |
|----------|-----------------|
| MeMe | 6.2 |
| EtEt | 2.3 |
| NonNon | 0.4 |
| PhePhe | 3.6 |
| MePhe | 4.3 |
| EtPhe | 1.4 |

More detailed gravimetric measurements revealed that the weight gain of dried EtEt³⁵ and of dried polyethyloxazoline–polyethersulfone blends³⁶ upon exposure to higher humidity equals the weight loss after subsequent drying. This reversibility supports the statement that water absorption is the cause for the observed softening.

Fig. 5 shows also that the type of indenter geometry used during the experiments (sphere or Berkovich) caused only minor differences. The comparison between the two indenter geometries and the two instruments is not explored further, as the current materials are not very suitable for these comparative investigations due to the dependency of the modulus on humidity.

The number of reports on the effect of humidity on the elastic modulus of glassy polymers is relatively small. This effect is reported for poly(methylmethacrylate) (PMMA) where E decreases by 0.44 GPa with an increase in RH from 0 to 100%,³⁷ and for polycarbonate (PC).³⁸ For (semicrystalline) ethylene–vinyl alcohol copolymers (29 mol% ethylene content) a drop in E from 3.0 to 1.9 GPa is reported upon a humidity increase from 0 to 53% RH;³⁹ for starch a drop from 2.4 to 1.5 GPa is reported for an increase from 32 to 90% RH.⁴⁰ Compared to these numbers, some of the drops in E_r reported in this work (for instance for PheMe) are surprisingly large.

Conclusions

Using depth-sensing indentation, for a diblock copoly(2-oxazoline) library the elastic moduli were screened in a HTE approach. No elastic moduli have been reported for these materials before. Depth-sensing indentation was successful, while sample preparation for standard macroscopic tensile or compression testing often fails for such brittle materials. At low RH, the homopolymers that were below their glass-transition temperature (methyl-, ethyl-, and phenyloxazoline) exhibited an elastic modulus E_r of 5 to 8.5 GPa. The E_r of the nonyloxazoline homopolymer (1.0 GPa) was lower, as the material was tested above its T_g . Crystallization of the nonyloxazoline prevented the modulus from decreasing into the range typical for amorphous polymers above T_g . The E_r of poly(ethyloxazoline) at low RH was low compared to poly(methyloxazoline) and poly(phenyloxazoline). The T_g of totally dry poly(ethyloxazoline) is only 34 °C above room temperature. Due to water uptake from the surrounding atmosphere, even at low RH, T_g is decreased and, as T_g approaches the temperature at which the measurements were performed, E_r is decreased as well. The E_r of poly(methyloxazoline) was higher than that expected for glassy polymers. This high E_r is attributed to hydrogen bonding or polar interactions between polymer chains. The E_r of AB diblock copolymers were between those of the A and B homopolymers. The E_r of copolymers with one poly(nonyloxazoline) block (~1.7 to 2.4 GPa at low RH) were closest to the E_r of poly(nonyloxazoline), which is consistent with the glassy phase being the minority volume fraction of such a copolymer. At higher humidities, the E_r of the poly(methyloxazoline) and poly(ethyloxazoline) decreased dramatically, which is caused by water uptake from the surrounding. The influence of

poly(oxazoline) side groups on the elastic modulus and on the response to humidity conditions provides interesting opportunities for tuning and optimizing polyoxazoline-based polymers for high performance applications which require, alongside other functionalities that copoly(oxazoline)s can offer, specific mechanical properties.

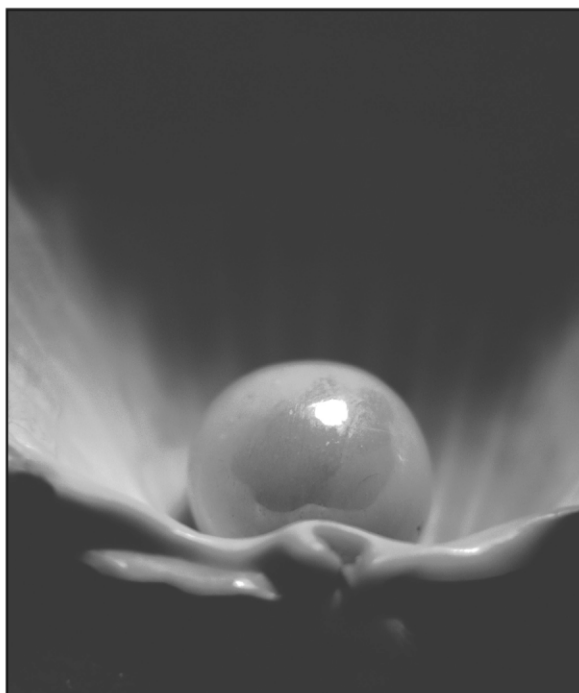
Acknowledgements

This research forms part of the research programme of the Dutch Polymer Institute (DPI), projects no. 496 and 543. JMK, CEH and USS gratefully acknowledge Hysitron, Inc. for discussions and support. CAT gratefully acknowledges the US National Science Foundation Graduate Fellowship. JMK, RH, CEH and USS thank Daan Wouters, Stephanie Hoepfener and Joe Delaney for helpful discussions and AFM and FTIR measurements.

References

- 1 M. A. R. Meier and U. S. Schubert, *J. Mater. Chem.*, 2004, **14**, 3289–3299.
- 2 B. Jandeleit, D. J. Schaefer, T. S. Powers, H. W. Turner and W. H. Weinberg, *Angew. Chem.*, 1999, **111**, 2648–2689, (*Angew. Chem., Int. Ed.*, 1999, **38**, 2494–2532).
- 3 O. L. Warren and Th. J. Wyrobek, *Meas. Sci. Technol.*, 2005, **16**, 100–110.
- 4 C. A. Tweedie, D. G. Anderson, R. Langer and K. J. Van Vliet, *Adv. Mater.*, 2005, **17**, 2599–2604.
- 5 W. C. Oliver and G. M. Pharr, *J. Mater. Res.*, 1992, **7**, 1564–1583.
- 6 M. R. Van Landingham, J. S. Villarrubia, W. F. Guthrie and G. F. Meyers, *Macromol. Symp.*, 2001, **167**, 15–43.
- 7 D. Delorme, Y. Ducharme, C. Brideau, C.-C. Chan, N. Chauret, S. Desmarais, D. Dube, J.-P. Falgouty, R. Fortin, J. Guay, P. Hamel, T. R. Jones, C. Lepine, C. Li, M. McAuliffe, C. S. McFarlane, D. A. Nicoll-Griffith, D. Riendeau, J. A. Yergey and Y. Girard, *J. Med. Chem.*, 1996, **39**, 3951–3970.
- 8 K. Aoi and M. Okada, *Prog. Polym. Sci.*, 1996, **21**, 151–208.
- 9 F. Wiesbrock, R. Hoogenboom, M. Leenen, S. F. G. M. van Nispen, M. van der Loop, C. H. Abeln, A. M. J. van den Berg and U. S. Schubert, *Macromolecules*, 2005, **38**, 7957–7966.
- 10 F. Wiesbrock, R. Hoogenboom, M. A. M. Leenen, M. A. R. Meier and U. S. Schubert, *Macromolecules*, 2005, **38**, 5025–5034.
- 11 R. Hoogenboom, M. W. M. Fijten and U. S. Schubert, *Macromol. Rapid Commun.*, 2004, **25**, 339–343.
- 12 S. Wijnands, B.-J. de Gans, F. Wiesbrock, R. Hoogenboom and U. S. Schubert, *Macromol. Rapid Commun.*, 2004, **25**, 1958–1962.
- 13 S. Hoepfener, F. Wiesbrock, R. Hoogenboom, H. M. L. Thijs and U. S. Schubert, *Macromol. Rapid Commun.*, 2006, **27**, 405–411.
- 14 J. L. Herz, A. J. Levy, M. H. Litt and J. L. Zuckerman, *Fr. Pat.*, 1 553 988, 1969. US Pat., 3 579 630, 1966.
- 15 A. J. Levy and M. H. Litt, *Fr. Pat.*, 1 560 117, 1969.
- 16 K. Edasawa and H. Saeki, *JP Pat.*, 2003–288508, 2003.
- 17 G. Cai, M. H. Litt and I. M. Krieger, *J. Polym. Sci., Part B: Polym. Phys.*, 1991, **29**, 773–784.
- 18 G. Cai and M. H. Litt, *J. Polym. Sci., Part A: Polym. Chem.*, 1996, **34**, 2689–2699.
- 19 G. Cai and M. H. Litt, *J. Polym. Sci., Part A: Polym. Chem.*, 1996, **34**, 2719–2727.
- 20 P. Van Caeter, E. J. Goethals, V. Gancheva and R. Velichkova, *Polym. Bull.*, 1997, **39**, 589–596.
- 21 S. Nuño-Donlucas, L. C. Cesteros, J. E. Puig and I. Katime, *Macromol. Chem. Phys.*, 2001, **202**, 663–671.
- 22 C. G. Simon, N. Eidelman, Y. Deng and N. R. Washburn, *Macromol. Rapid Commun.*, 2004, **25**, 2003–2007.
- 23 W. C. Oliver and G. M. Pharr, *J. Mater. Res.*, 2004, **19**, 3–20.
- 24 A. C. Fisher-Cripps, *Nanoindentation*, Springer, New York, 2nd edn, 2004.
- 25 Y.-T. Cheng and C.-M. Cheng, *Mater. Sci. Eng., R*, 2004, **44**, 91–149.
- 26 G. Feng and A. H. W. Ngan, *J. Mater. Res.*, 2002, **17**, 660–668.

- 27 R. Hoogenboom, M. W. M. Fijten, H. M. L. Thijs, B. M. van Lankvelt and U. S. Schubert, *Des. Monomers Polym.*, 2005, **8**, 659–671.
- 28 L. S. A. Smith and V. Schmitz, *Polymer*, 1988, **29**, 1871–1878.
- 29 R. J. Young and P. A. Lovell, *Introduction to polymers*, Chapman & Hall, London, 2nd edn, 1991.
- 30 J. Brandrup, E. H. Immergut and E. A. Grulke, *Polymer Handbook*, John Wiley & Sons, New York, 4th edn, 1999.
- 31 B. J. Briscoe, L. Fiori and E. Pelillo, *J. Phys. D: Appl. Phys.*, 1998, **31**, 2395–2405.
- 32 P. V. Pavoov, A. Bellare, A. Strom, D. Yang and R. E. Cohen, *Macromolecules*, 2004, **37**, 4865–4871.
- 33 M. Nowicki, A. Richter, B. Wolf and H. Kaczmarek, *Polymer*, 2003, **44**, 6599–6606.
- 34 A. Bolshakov and G. M. Pharr, *J. Mater. Res.*, 1998, **13**, 1049–1058.
- 35 H. M. L. Thijs, C. R. Becer, D. Fournier, R. Hoogenboom and U. S. Schubert, in preparation.
- 36 K. A. Schult and D. R. Paul, *J. Polym. Sci., Part B: Polym. Phys.*, 1997, **35**, 993–1007.
- 37 C. Ishiyama and Y. Higo, *J. Polym. Sci., Part B: Polym. Phys.*, 2002, **40**, 460–465.
- 38 F. P. La Mantia, G. Spadaro and D. Acierno, *Acta Polym.*, 1981, **32**, 209–211.
- 39 L. Cabedo, J. M. Lagarón, D. Cava, J. J. Saura and E. Giménez, *Polym. Test.*, 2006, **25**, 860–867.
- 40 S. Mali, L. S. Sakanaka, F. Yamashita and M. V. E. Grossman, *Carbohydr. Polym.*, 2005, **60**, 283–289.



Looking for that **special** chemical biology research paper?

TRY this free news service:

Chemical Biology

- highlights of newsworthy and significant advances in chemical biology from across RSC journals
- free online access
- updated daily
- free access to the original research paper from every online article
- also available as a free print supplement in selected RSC journals.*

*A separately issued print subscription is also available.

Registered Charity Number: 207890

RSCPublishing

www.rsc.org/chembiology

22030681